Performance of Compressed Sensing MIMO Radar Based on Low-Rank Matrix Recovery

Byron McMullen and Seung-Jun Kim
Dept. of Computer Science & Electrical Engineering
University of Maryland, Baltimore County
Baltimore, MD, 21250, USA
E-mails: {mcmulby1,sjkim}@umbc.edu

***Abstract*—Compressed sensing (CS) techniques have been successfully applied to multi-input multi-output (MIMO) radars to drastically reduce the sampling rates required for acquiring data. In this work, a CS MIMO radar is derived by employing a matrix recovery algorithm exploiting the low-rank structure of the data matrix based on linearly compressed measurements. Compared to a MIMO radar based on low-rank matrix completion, the proposed approach is seen to provide superior data reconstruction and target estimation performance at lower sampling rates.**

***Index Terms*—MIMO radar, low-rank matrix recovery, random modulator pre-integrator, compressed sensing.**

I. Introduction

Recently, compressive sampling (CS) techniques have been applied to MIMO radar signal processing, allowing drastically reduced sampling rates, without sacrificing the radar performance. A CS MIMO radar was developed by exploiting the sparsity of the radar scene and the bounds for the range and azimuth resolution, as well as the number of recoverable targets were derived [1]. The CS technique was employed assuming that the targets are sparse in the angle-Doppler domain, and the recovery algorithm was implemented based on ℓ_1-norm minimization to achieve high-resolution estimation with much fewer samples than a traditional MIMO radar in [2]. A typical limitation in the sparsity-based CS MIMO radar is that the estimated parameter space needs to be discretized, which incurs errors when the targets are not well aligned with the grid points.

It has also been recognized that a CS MIMO radar can be developed based on the low-rank structure of the data matrix. In [4], at each receive antenna element, either randomly switched matched filtering or sub-Nyquist-rate random sampling is performed, and the samples are forwarded to a fusion center, resulting in a data matrix with missing entries. Then, the entire data matrix is reconstructed through matrix completion (MC) based on the low-rank property. This MIMO-MC radar does not require discretization of the parameter space and was shown to provide high-resolution estimates at a low sampling rate. In [5], MC was applied to a MIMO radar system with a shared receive array. When the received signal is only partially observed due to receiver sharing, the missing entries are imputed by exploiting the correlation of successive data matrices through dynamic MC. It was shown that the MC algorithm can also improve the signal quality due to the denoising effect. MC was also applied to MIMO radar using a sparse planar array, where the sparsity of the array was induced by randomly removing individual elements or entire rows/columns [6]. In order to guarantee that the low-rank property held, the original matrix was reconstructed into a two-fold Hankel structure. The MC technique was also used for meteorological remote sensing and target estimation applications [7], [8].

In this work, a CS MIMO radar is developed based on the low-rank property of the data matrix, but random linear projections of the received signal are used as measurements. In particular, the random modulator pre-integrator (RMPI) architecture, which was shown effective for CS data acquisition systems, is adopted [9], [10]. Then, the entire data matrix is recovered based on low-rank matrix recovery using a nuclear norm minimization formulation. The resulting RMPI MIMO radar shows excellent performance in data matrix recovery and target parameter estimation, outperforming the MC-based MIMO radar especially when the effective sampling rate is much lower than the Nyquist rate.

The rest of the paper is organized as follows. The MIMO radar signal model is presented in Sec. II. The compressive sensing scheme and the data matrix recovery are described in Sec. III. The results of performance evaluation are discussed in Sec. IV. The conclusion is provided in Sec. V.

II. Signal Model

A standard model for a MIMO pulsed radar system with collocated transmit and receive antennas is adopted [3], [4]. The transmit and receive antennas, which are stationary, are uniform linear arrays (ULAs) having M_T and M_R elements, respectively. The inter-element spacings of the transmit and receive arrays are denoted as d_T and d_R, respectively. The radar system transmits Q pulses, each of duration T_P with energy E. The pulse repetition interval (PRI) of the pulses is T_{PRI}. Let τ be the time within each pulse satisfying $0 \leq \tau \leq T_P$. The m-th element in the transmit array emits an orthogonal baseband waveform $s_m(\tau) := \sqrt{E}\phi_m(\tau)$ with $\int \phi_m(\tau)\phi_k^*(\tau)d\tau = \delta_{mk}$, for $m, k \in \{0, 1, \ldots, M_T - 1\}$, where * denotes complex conjugation, and $\delta_{mk} = 1$ if $m = k$

and 0 otherwise. The modulated waveform $\tilde{s}_m(t)$ that is transmitted over carrier frequency f can be expressed as

$$\tilde{s}_m(qT_{PRI}+\tau) = \sqrt{E}\phi_m(\tau)e^{j2\pi f(qT_{PRI}+\tau)}, \quad q=0,1,\ldots,Q-1,\ 0\le\tau\le T_P. \tag{1}$$

Suppose that there are K targets, with the k-th target located at range R and azimuth angle θ_k, moving at a radial velocity v_k, having a complex reflection coefficient β_k, for $k=1,2,\ldots,K$. Let λ be the wavelength of the carrier given by $\lambda=\frac{c}{f}$, where c is the speed of light. Then, the signal transmitted by the m-th transmit antenna, reflected by the k-th target, and received by the n-th receive antenna, can be expressed as

$$\tilde{s}_m\left(qT_{PRI}+\tau+\frac{2R}{c}\right) \cdot \beta_k e^{j\frac{2\pi}{\lambda}(nd_R\sin\theta_k+md_T\sin\theta_k)}e^{j\frac{2\pi}{\lambda}2v_kqT_{PRI}}. \tag{2}$$

For simplicity, let us assume that the transmit waveforms $s_m(t)$ are narrowband, and the target reflection coefficients β_k are constant over all pulses. Furthermore, the delay spread in the received signals is assumed to be much smaller than the pulse duration T_P, and the Doppler spread $\frac{2v_k}{\lambda}$ much smaller than the pulse bandwidth $1/T_P$. Moreover, it is assumed that the Doppler shift in the fast time can be neglected, resulting in the Doppler shift depending only on the slow time pulse index q [4].

Under these assumptions, the demodulated signal $x_l(t)$ observed by the l-th receive antenna during the q-th pulse interval can be written as

$$x_l\left(qT_{PRI}+\tau+\frac{2R}{c}\right) \approx w_l\left(qT_{PRI}+\tau+\frac{2R}{c}\right) + \sum_{k=1}^{K}\sum_{m=0}^{M_T-1}\sqrt{E}\phi_m(\tau)\beta_k e^{j\frac{2\pi}{\lambda}\sin\theta_k(ld_R+md_T)}e^{j\frac{2\pi}{\lambda}2v_kqT_{PRI}}, \quad l=0,\ldots,M_R-1 \tag{3}$$

where $w_l(t)$ contains both noise and interference. Eq. (3) can be simplified by introducing the steering vector $\mathbf{a}(\theta_k)$ of the transmit array toward the k-th target, given by

$$\mathbf{a}(\theta_k) := [1, e^{j\frac{2\pi}{\lambda}d_T\sin\theta_k}, ..., e^{j\frac{2\pi}{\lambda}(M_T-1)d_T\sin\theta_k}]^\top \tag{4}$$

where $^\top$ denotes transposition. Similarly, define the steering vectors of the receive array as

$$\mathbf{b}(\theta_k) := [1, e^{j\frac{2\pi}{\lambda}d_R\sin\theta_k}, ..., e^{j\frac{2\pi}{\lambda}(M_R-1)d_R\sin\theta_k}]^\top. \tag{5}$$

Define also $\mathbf{s}(\tau) := [s_0(\tau),\ldots,s_{M_T-1}(\tau)]^\top$. Then, $x_l(t)$ can be expressed as

$$x_l\left(qT_{PRI}+\tau+\frac{2R}{c}\right) \approx w_l\left(qT_{PRI}+\tau+\frac{2R}{c}\right) + \sum_{k=1}^{K}\beta_k e^{j\frac{2\pi}{\lambda}ld_R\sin\theta_k}e^{j\frac{2\pi}{\lambda}2v_kqT_{PRI}}\mathbf{a}(\theta_k)^\top\mathbf{s}(\tau). \tag{6}$$

The samples of $x_l(t)$ will be acquired using a sub-Nyquist rate sampling device, as will be discussed in Sec. III. For now,

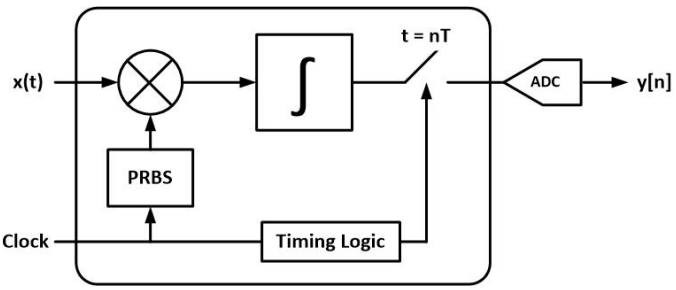

Fig. 1. Block diagram for RMPI.

if each element in the antenna array were to be sampled at the Nyquist sampling rate f_{Nyq}, the N samples over the q-th pulse obtained from the l-th antenna element can be expressed as

$$\mathbf{x}_{ql} := \left[x_l\left(qT_{PRI}+\tfrac{2R}{c}\right),\ldots,x_l\left(qT_{PRI}+\tfrac{N-1}{f_{Nyq}}+\tfrac{2R}{c}\right)\right]^\top. \tag{7}$$

Collecting the samples from M_R antennas, the data matrix for the q-th pulse can then be defined as

$$\mathbf{X}_q := [\mathbf{x}_{q0},\ldots,\mathbf{x}_{q,(M_R-1)}]^\top \in \mathbb{C}^{M_R\times N}. \tag{8}$$

Now let

$$\mathbf{A} := [\mathbf{a}(\theta_1),\ldots,\mathbf{a}(\theta_K)] \in \mathbb{C}^{M_T\times K} \tag{9}$$

$$\mathbf{B} := [\mathbf{b}(\theta_1),\ldots,\mathbf{b}(\theta_K)] \in \mathbb{C}^{M_R\times K} \tag{10}$$

$$\mathbf{\Sigma} := \mathrm{diag}\{\beta_1,\ldots,\beta_K\} \tag{11}$$

$$\mathbf{D}_q := \mathrm{diag}\{e^{j\frac{2\pi}{\lambda}2v_1(q-1)T_{PRI}},\ldots,e^{j\frac{2\pi}{\lambda}2v_K(q-1)T_{PRI}}\} \tag{12}$$

$$\mathbf{S} := [\mathbf{s}(0),\ldots,\mathbf{s}((N-1)/f_{Nyq})] \in \mathbb{C}^{M_T\times N}. \tag{13}$$

Finally, let $\mathbf{W}_q \in \mathbb{C}^{M_R\times N}$ be the matrix whose $(l+1,n+1)$-entry for $l=0,\ldots,M_R-1$ and $n=0,\ldots,N-1$ is equal to $w_l(qT_{PRI}+n/f_{Nyq}+2R/c)$. Then, it can be easily verified that

$$\mathbf{X}_q = \mathbf{B}\mathbf{\Sigma}\mathbf{D}_q\mathbf{A}^\top\mathbf{S}+\mathbf{W}_q. \tag{14}$$

Therefore, provided that $\min\{K,M_T\}\ll\min\{M_R,N\}$, the rank of the noise-free data matrix $\mathbf{Z}_q := \mathbf{B}\mathbf{\Sigma}\mathbf{D}_q\mathbf{A}^\top\mathbf{S}$ is $\min\{K,M_T\}$ and $\mathbf{Z}_q$ is low-rank [4].

III. Compressive Sensing and Recovery

To acquire sub-Nyquist rate compressive samples, the random-modulation pre-integrator (RMPI) architecture is employed [9], [10]. The RMPI is an analog-to-information (A2I) converter that has been shown to provide simple and efficient compression for data acquisition systems. The input is processed by a random demodulator (RD) based on a pseudo-random bit sequences (PRBSs), followed by integration and sampling. The pipeline provides a channel of outputs, and multiple channels are often implemented. Fig. 1 shows the RMPI architecture with a single channel.

More specifically, consider an input signal $x(\tau)$ and a chipping signal $c(\tau)$ of duration T_P. Then, for a positive

integer M with $T_{int} := T_P/M$, the RMPI obtains the i-th sample by integrating the modulated signal $x(\tau)c(\tau)$ as

$$y[i] = \int_{iT_{int}}^{(i+1)T_{int}} x(\tau)c(\tau)d\tau,\ i = 0, \ldots, M-1. \quad (15)$$

The chipping signal $c(\tau)$ is generated using a PRBS taking values ± 1 with equal probabilities and toggling at a rate of f_{chip}. In order to efficiently capture signals with bandwidth B, it is necessary to have $f_{chip} \geq f_{Nyq} = 2B$. To simply the exposition, let us assume here that $f_{chip} = f_{Nyq}$ and a rectangular pulse of duration $1/f_{chip}$ is used for the chip waveform. Furthermore, assume that $T_P f_{Nyq}$ is an integer equal to N, and $N_{int} := N/M$ is also an integer.

Suppose that the input $x(\tau) = x_l(qT_{PRI} + \tau + 2R/c)$. Then, one can relate the Nyquist-rate samples $\mathbf{x}_{ql}$ to the sub-Nyquist rate samples obtained from the RMPI. For this, define a diagonal matrix of the PRBS $\{c_n^{(l,p)} \in \{-1, 1\}\}_{n=0}^{N-1}$ for receive antenna l and RMPI channel p as

$$\mathbf{C}^{(l,p)} := \mathrm{diag}\{c_0^{(l,p)}, \ldots, c_{N-1}^{(l,p)}\},$$
$$l = 0, \ldots, M_R - 1,\ p = 1, \ldots, N_{ch} \quad (16)$$

where the PRBS is unique for each of N_{ch} channels. Define also the matrix that represents the integration and the sampling operations as

$$\mathbf{H} := \mathbf{I}_M \otimes \underbrace{[1, 1, \ldots, 1]}_{N_{int}} \in \{0, 1\}^{M \times N} \quad (17)$$

where $\mathbf{I}_M$ is an $M \times M$ identity matrix and $\otimes$ denotes the Kronecker product. Let $\mathbf{y}_{ql}^{(p)} \in \mathbb{C}^M$ be the vector of samples from the RMPI [cf. (15)], and

$$\mathbf{y}_{ql} := [\mathbf{y}_{ql}^{(1)\top}, \ldots, \mathbf{y}_{ql}^{(N_{ch})\top}]^\top \in \mathbb{C}^{N_{ch}M}. \quad (18)$$

Then, upon defining

$$\mathbf{\Phi}_l := \begin{bmatrix} \mathbf{H}\mathbf{C}^{(l,1)} \\ \vdots \\ \mathbf{H}\mathbf{C}^{(l,N_{ch})} \end{bmatrix} \in \{-1, 1\}^{N_{ch}M \times N} \quad (19)$$

it can be seen that $\mathbf{y}_{ql} = \mathbf{\Phi}_l \mathbf{x}_{ql}$.

This process can be repeated for all receive antenna elements. Collecting $\mathbf{y}_{ql}$ for $l = 0, \ldots, M_R - 1$, one can obtain the compressive sample vector $\mathbf{y}_q := [\mathbf{y}_{q0}^\top, \ldots, \mathbf{y}_{q,M_R-1}^\top]^\top \in \mathbb{C}^{N_{ch}MM_R}$. Then, it can be easily seen that

$$\mathbf{y}_q = \mathrm{bdiag}\{\mathbf{\Phi}_0, \ldots, \mathbf{\Phi}_{M_R-1}\}\mathrm{vec}(\mathbf{X}_q^\top) \quad (20)$$
$$= \mathcal{A}(\mathbf{X}_q) = \mathcal{A}(\mathbf{Z}_q) + \mathcal{A}(\mathbf{W}_q) \quad (21)$$

where $\mathrm{bdiag}\{\cdot\}$ constructs a block-diagonal matrix by arranging the matrices in $\{\cdot\}$ consecutively, $\mathrm{vec}(\cdot)$ vectorizes a matrix by stacking its columns, and $\mathcal{A} : \mathbb{C}^{M_R \times N} \to \mathbb{C}^{N_{ch}MM_R}$ is a linear mapping defined implicitly from (20)–(21). Note that $\mathcal{A}$ compresses the Nyquist rate data matrix of dimension $M_R \times N$ to a vector of dimension $N_{ch}MM_R$, reducing the sampling rate effectively to

$$f_s := f_{Nyq}\frac{N_{ch}M}{N}\ \text{[samples per second]}. \quad (22)$$

To recover the Nyquist-rate data matrix $\mathbf{Z}_q$ from compressive samples $\mathbf{y}_q$, low-rank matrix recovery (LRMR) is performed based on (20)–(21). In particular, the following nuclear norm minimization problem is solved [11].

$$\text{minimize } \|\mathbf{Z}_q\|_* \quad (23a)$$
$$\text{subject to } \|\mathbf{y}_q - \mathcal{A}(\mathbf{Z}_q)\|_2 \leq \epsilon \quad (23b)$$

where $\|\cdot\|_*$ denotes the nuclear norm (the sum of singular values), which is a convex surrogate for matrix rank, and ϵ is a parameter related to noise magnitude. Problem (23) can be solved efficiently using various methods including the alternating direction method of multipliers (ADMM) [12].

IV. Performance Evaluation

A. Experiment Setup

To evaluate the performance, a MIMO radar system with $M_T = M_R = 20$ is considered. The inter-element spacing is $d_T = d_R = \frac{\lambda}{2}$. The transmitter emits a set of Hadamard waveforms of length $N = 512$ at carrier frequency $f = 1$ GHz. The number of pulses transmitted is $Q = 3$ and the pulse repetition frequency (PRF) is 6 kHz. The number of targets is set to $K = 3$. The targets were assigned with azimuth angles in $[-90°, 90°]$ with velocities in $[-450, 450]$ m/s. The complex reflection coefficients of the targets were generated randomly. Zero-mean Gaussian noise was introduced at the receive antennas. For comparison, the matrix completion (MC)-based MIMO-MC radar [4] was also implemented. The average results are obtained from 100 Monte Carlo runs.

B. Data Matrix Recovery Performance

First, the performance of the data matrix recovery of the RMPI-based MIMO radar is evaluated at various compression rates and signal-to-noise power ratio (SNR) levels. The compression rate is defined as

$$\left(1 - \frac{N_{ch}M}{N}\right) \times 100\ [\%]. \quad (24)$$

As the performance metric, the normalized mean square error (NMSE) between the true data matrix $\mathbf{Z}_q$ and the estimated one $\hat{\mathbf{Z}}_q$, defined by

$$\mathrm{NMSE} := \frac{\|\hat{\mathbf{Z}}_q - \mathbf{Z}_q\|_F}{\|\mathbf{Z}_q\|_F} \quad (25)$$

is used, where $\|\cdot\|_F$ denotes the Frobenius norm. Fig. 2 shows the NMSE performances of the RMPI MIMO radar at compression rates $\{25\%, 50\%, 75\%, 87.5\%, 90.6\%\}$ and SNRs 0–60 dB. For comparison, the NMSEs of the MIMO-MC radar are also depicted. It can be seen that, at low compression rates, the two schemes perform similarly. However, the RMPI MIMO radar performs markedly better at compression rates equal to or larger than 75%.

C. Target Parameter Estimation Performance

To assess the target parameter estimation performance of the radar, a subspace-based algorithm is adopted for joint angle and velocity estimation as in [4]. Let $\hat{\mathbf{Z}}_q$ denote the estimated data matrix during pulse q. Noting that $\frac{T_P}{EN}\mathbf{S}\mathbf{S}^H = \mathbf{I}$, where $\cdot^H$ denotes Hermitian transpose, one can perform matched filtering on $\hat{\mathbf{Z}}_q$ to get

$$\mathbf{Y}_q := \frac{T_P}{EN}\hat{\mathbf{Z}}_q\mathbf{S}^H = \mathbf{B}\mathbf{\Sigma}\mathbf{D}_q\mathbf{A}^\top + \tilde{\mathbf{W}}_q \tag{26}$$

where $\tilde{\mathbf{W}}_q$ represents the noise matrix that is a function of both the noise due to the radar receiver and the recovery error. By collecting $\mathbf{Y}_q$ for $q = 0, \ldots, Q-1$, form $\tilde{\mathbf{Y}} := [\mathbf{Y}_0, \ldots, \mathbf{Y}_{Q-1}]^\top \in \mathbb{C}^{QM_T \times M_R}$. Upon defining

$$\mathbf{F} := [\mathbf{d}(v_1) \otimes \mathbf{a}(\theta_1), \ldots, \mathbf{d}(v_K) \otimes \mathbf{a}(\theta_K)] \tag{27}$$

$$\mathbf{d}(v) := [1, e^{j\frac{2\pi}{\lambda}2vT_{PRI}}, \ldots, e^{j\frac{2\pi}{\lambda}2v(Q-1)T_{PRI}}] \tag{28}$$

it can be shown that [4]

$$\tilde{\mathbf{Y}} = \mathbf{F}\mathbf{\Sigma}\mathbf{B}^\top + \tilde{\mathbf{W}} \tag{29}$$

where $\tilde{\mathbf{W}} := [\tilde{\mathbf{W}}_0, \ldots, \tilde{\mathbf{W}}_{Q-1}]^\top$. The sample covariance matrix $\hat{\mathbf{R}}_{\tilde{Y}}$ of $\tilde{\mathbf{Y}}$ can be computed as

$$\hat{\mathbf{R}}_{\tilde{Y}} = \frac{1}{M_R}\tilde{\mathbf{Y}}\tilde{\mathbf{Y}}^H. \tag{30}$$

For joint angle and velocity estimation, a two-dimensional MUSIC estimator performs an eigenanalysis of $\hat{\mathbf{R}}_{\tilde{Y}}$ to obtain the noise subspace $\mathbf{E}_n$ corresponding to the $(QM_T - K)$ smallest eigenvalues. The azimuth angles and velocities of the targets can be obtained by finding the peak locations of the MUSIC pseudospectrum given by

$$P(\theta, v) = \frac{1}{(\mathbf{d}(v) \otimes \mathbf{a}(\theta))^H \mathbf{E}_n \mathbf{E}_n^H (\mathbf{d}(v) \otimes \mathbf{a}(\theta))}. \tag{31}$$

Fig. 3 shows the pseudospectra based on the ground truth data matrix $\mathbf{Z}_q$ (top), the estimated data matrix $\hat{\mathbf{Z}}_q$ using RMPI MIMO radar (middle), and the estimated data matrix using MIMO-MC radar (bottom), at 75% compression and 10 dB SNR. It is clear that the pseudospectrum for the MIMO-MC radar undergoes excessive spreading in the angle-velocity domain. Also notice that the peak values at the target locations are much smaller than those from the RMPI MIMO radar, which indicates that the RMPI radar estimates are more robust.

Fig. 4 shows the mean velocity errors at different compression rates and SNR levels. It is clear that the RMPI MIMO radar offers better target parameter estimation performance than the MIMO-MC radar especially when the compression rate is high.

V. Conclusion

A compressive sensing MIMO radar is proposed using low-rank matrix recovery. The RMPI architecture is adopted to obtain sub-Nyquist rate samples of the received signals at the antenna array, and the Nyquist-rate data matrix was recovered through a nuclear norm minimization formulation based on the low-rank property. Compared to the MIMO-MC radar that performs low-rank matrix completion, it was seen from the numerical tests that the RMPI MIMO radar obtains the data matrix with smaller NMSE when the compression rate exceeds 50%. Furthermore, the target velocity estimation performance of the RMPI MIMO radar was seen to be superior to that of the MIMO-MC radar, especially when the undersampling is aggressive. Further experimental tests and theoretical analysis of the recovery guarantee are planned for future work.

References

[1] T. Strohmer and B. Friedlander, "Compressed sensing for MIMO radar - algorithms and performance," in *Proc. of the 43rd Asilomar Conf. on Signals, Syst. and Comput.*, Pacific Grove, CA, Nov. 2009, pp. 464–468.

[2] Y. Yu, A. P. Petropulu and H. V. Poor, "MIMO radar using compressive sampling," *IEEE J. Sel. Topics Signal Process.*, vol. 4, no. 1, pp. 146–163, Feb. 2010.

[3] D. Nion and N. D. Sidiropoulos, "Tensor algebra and multidimensional harmonic retrieval in signal processing for MIMO radar," *IEEE Trans. Signal Process.*, vol. 58, no. 11, pp. 5693–5705, Nov. 2010.

[4] S. Sun, W. U. Bajwa and A. P. Petropulu, "MIMO-MC radar: A MIMO radar approach based on matrix completion," *IEEE Trans. Aerosp. Electron. Syst.*, vol. 51, no. 3, pp. 1839–1852, Jul. 2015.

[5] H. Vardhan, R. Tripathi and K. Rajawat, "Adaptive front-end for MIMO radar with dynamic matrix completion," in *Proc. Int. Conf. Signal Process. and Commun.*, Bangalore, India, Jul. 2020, pp. 1–5.

[6] X. Hu, N. Tong, J. Wang, S. Ding, X. Zhao, "Matrix completion-based MIMO radar imaging with sparse planar array," *Signal Process.*, vol. 131, pp. 49–57, Feb. 2017.

[7] K. V. Mishra, A. Kruger, and W. F. Krejewski, "Compressed sensing applied to weather radar," *Proc. IEEE Geosci. Remote Sensing Symp.*, Quebec City, QC, Nov. 2014, pp. 1832–1835.

[8] S. Sun, K. V. Mishra, and A. P. Petropulu, "Target estimation by exploiting low rank structure in widely separated MIMO radar," *Proc. IEEE Radar Conf.*, Boston, MA, Apr. 2019.

[9] J. Yoo, *Compressed Sensing Receivers: Theory, Design, and Performance Limits.* Ph.D. Dissertation, Calif. Inst. of Technol., 2012.

[10] J. A. Tropp, J. N. Laska, M. F. Duarte, J. K. Romberg and R. G. Baraniuk, "Beyond Nyquist: Efficient sampling of sparse bandlimited signals," *IEEE Trans. Inf. Theory*, vol. 56, no. 1, pp. 520–544, Jan. 2010.

[11] S. Oymak, K. Mohan, M. Fazel and B. Hassibi, "A simplified approach to recovery conditions for low rank matrices," in *Proc. IEEE Int. Symp. Info. Theory*, St. Petersburg, Russia, Jul. 2011, pp. 2318–2322.

[12] A. Gogna, A. Shukla and A. Majumdar, "Matrix recovery using split Bregman," in *Proc. of the 22nd Int. Conf. on Pattern Recognit.*, Stockholm, Sweden, Aug. 2014, pp. 1031–1036.

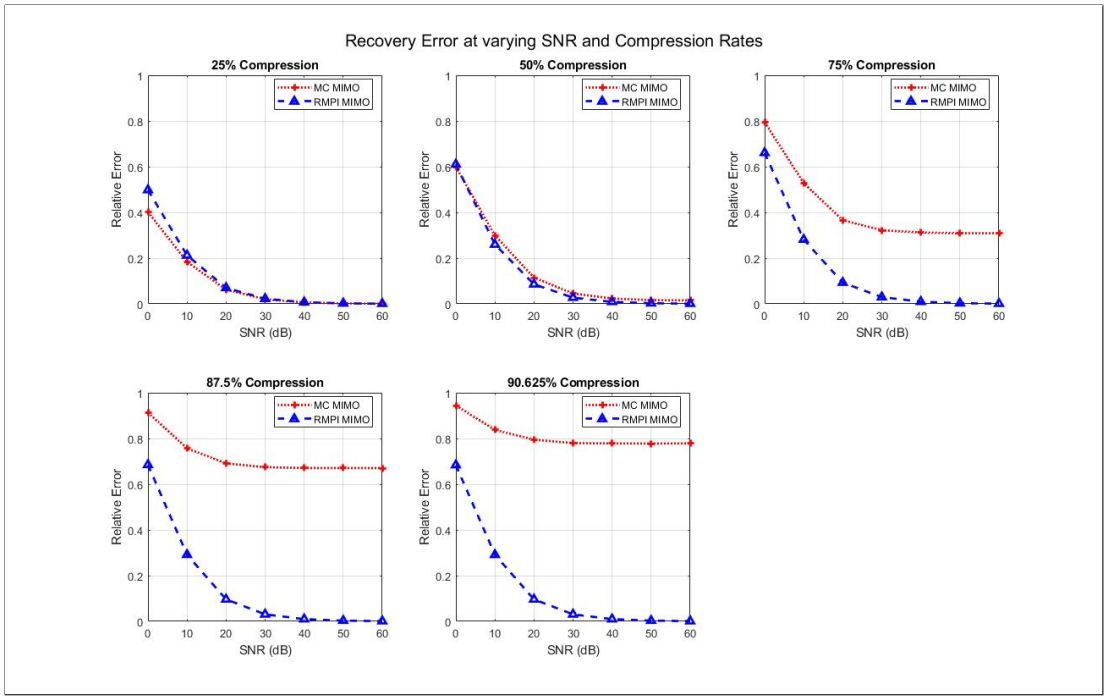

Fig. 2. NMSE versus SNR for different compression rates.

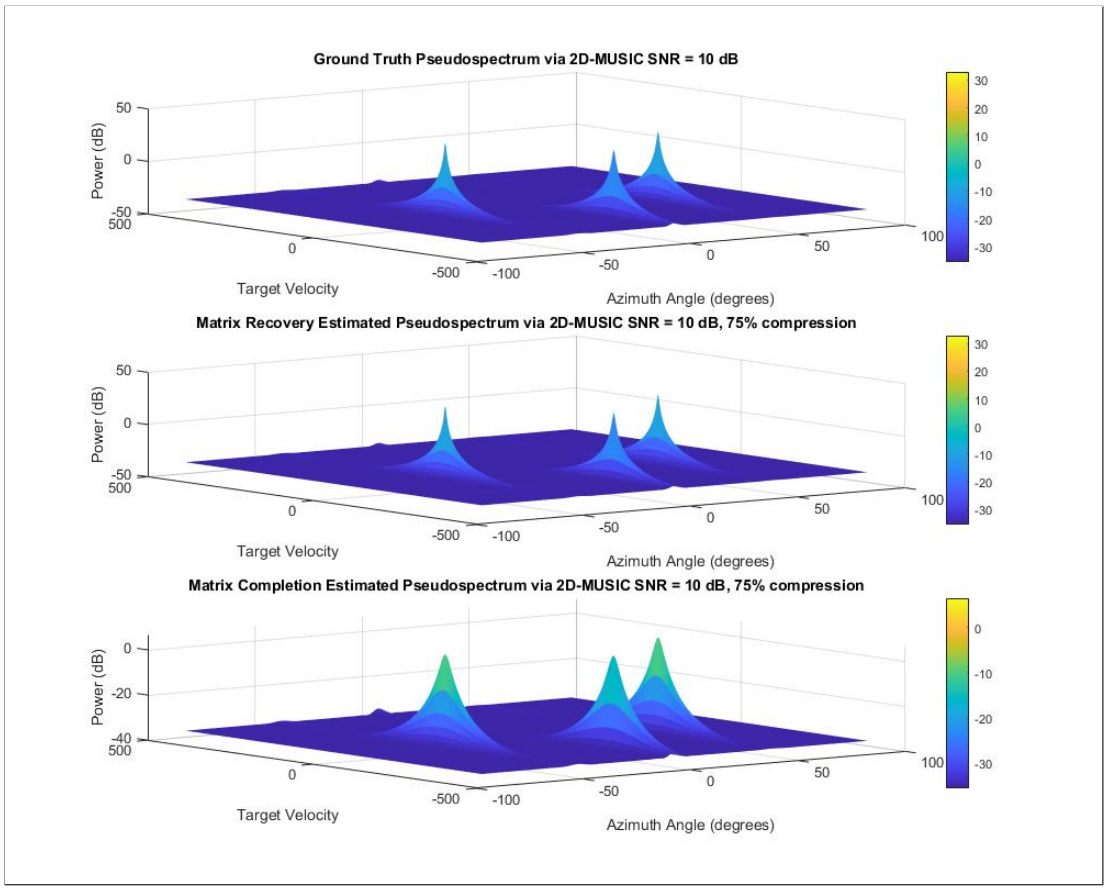

Fig. 3. MUSIC pseudospectra at 75% compression and 10 dB SNR.

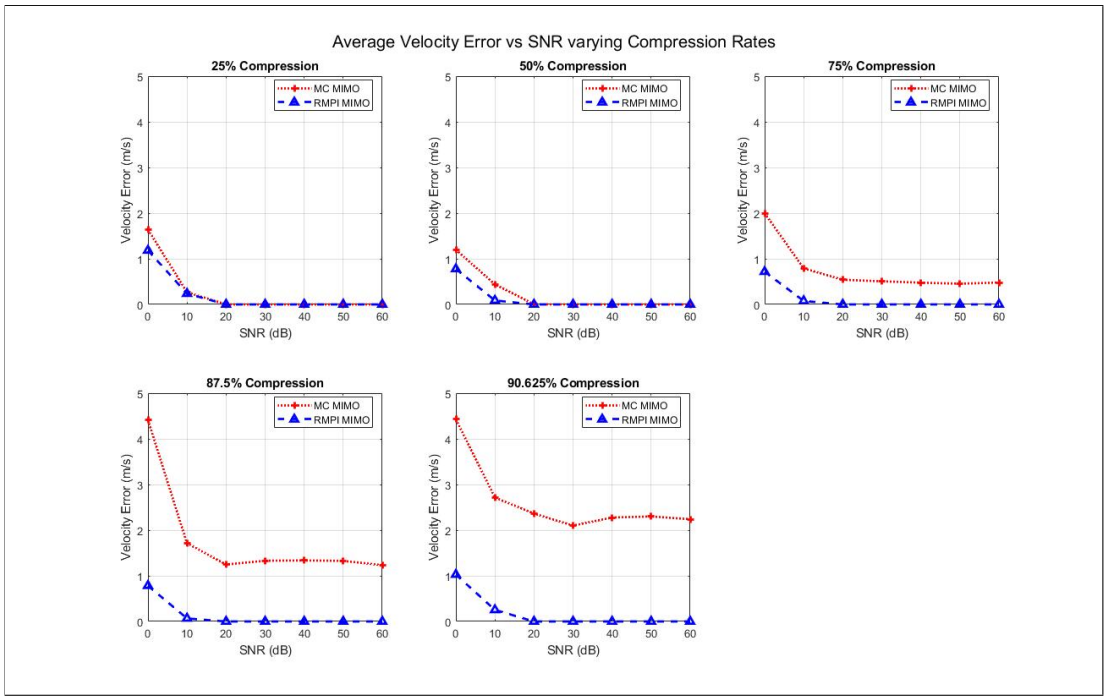

Fig. 4. Average velocity estimation error versus SNR at various compression rates.